

Preparations, structures and photolyses of peralkyldisilagermirane and peralkylgermadisilaoxetane

Hideo Suzuki^a, Kazutoshi Okabe^a, Satoshi Uchida^a, Hamao Watanabe^{a,*}, Midori Goto^{b,*}

^a Department of Chemistry (Materials Science), Faculty of Engineering, Gunma University, Kiryu, Gunma 376, Japan

^b National Institute of Materials and Chemical Research, Tsukuba, Ibaraki 305, Japan

Received 27 April 1995; in revised form 21 June 1995

Abstract

Three- and four-membered ring systems, peralkyldisilagermirane ($[\text{R}_2\text{Si}]_2\text{GeR}'_2$ (**1**)) and peralkylgermadisilaoxetane ($[\text{R}_2\text{SiGeR}'_2\text{SiR}_2]\text{O}$ (**2**)) ($\text{R} = \text{tBuCH}_2$; $\text{R}' = \text{Me}_3\text{SiCH}_2$) respectively were synthesized and characterized. The structures of **1** and **2** have been determined by X-ray crystallography. The ring of GeSi_2O (**2**) is almost planar. The photolysis of **1** and **2** using a mercury lamp ($\lambda = 254 \text{ nm}$) gave mainly disilene and disilaoxirane respectively with extrusion of germylene.

Keywords: Disilagermirane; Germadisilaoxetane; X-ray structure; Photolysis

1. Introduction

Much attention has been focused on the chemistry of highly strained compounds of cyclometallanes, especially cyclotrisilanes (Si_3) and cyclotrigermanes (Ge_3), which provide intriguing subjects because of their unusual properties and structures. Recently, the synthesis and characterization of a few compounds containing mixed cyclotrimetallane ring systems, namely $[(\text{Me}_3\text{Si})_2\text{Si}]_2\text{Ge}(\text{SiMe}_3)_2$ [**1**] and $[\text{Mes}_2\text{Ge}]_2\text{SiMes}_2$ [**2a**], have been reported. Subsequently, the studies regarding their molecular structures, thermodynamics [**2**] and reactivities including theoretical calculations of the model ring systems $[\text{H}_2\text{Si}]_2\text{GeH}_2$ and $[\text{H}_2\text{Ge}]_2\text{SiH}_2$ [**3**] have also been described. However, there are no reports on the study of compounds which consist of peralkylated mixed-trimetallane ring systems. It is of great importance and interest to study the physical and chemical properties of the usual peralkylated Si_2Ge ring compounds to assess the electronic properties of the cyclometallane systems, since the above types of compound which have rather particular substituents such as trimethylsilyl and mesityl groups are not convenient because of the perturbation caused by these substituents on the ring metals.

We have previously studied some properties of a variety of peralkylated cyclosilanes, $[\text{R}^1\text{R}^2\text{Si}]_n$ ($n = 3-7$) [**4**] and $[\text{R}_2\text{Si}]_n\text{O}$ ($n = 3$) [**5**]. Recently we reported the synthesis and the molecular structure of the four-membered Si_3Ge ring systems $[\text{R}_2\text{Si}]_3\text{Ge}(\text{CH}_2\text{SiMe}_3)_2$ ($\text{R} = \text{tBuCH}_2$ (**A**) or tPr (**B**)) [**6**] and subsequently we also reported that the photolysis of **A** and **B** affords cyclotrisilanes with extrusion of germylene [**7**]. In our continuing interest in the synthesis and photochemical behavior of small-membered cyclosilanes bearing alkyl groups on ring metals, we now should like to report the syntheses and photolyses of 1,1-bis(trimethylsilylmethyl)-2,2,3,3-tetraneopentyl-1-germa-2,3-disilacyclopropane ($[\text{R}_2\text{Si}]_2\text{GeR}'_2$ (**1**)) and the related 3,3-bis(trimethylsilylmethyl)-2,2,4,4-tetraneopentyl-1-oxa-3-germa-2,4-disilacyclobutane ($[\text{R}_2\text{SiGeR}'_2\text{SiR}_2]\text{O}$ (**2**)) ($\text{R} = \text{tBuCH}_2$, $\text{R}' = \text{Me}_3\text{SiCH}_2$) and the molecular structures of the two compounds via X-ray crystal analysis.

2. Results and discussion

2.1. Preparation of **1** and **2**

Compound **1** was obtained with a good yield (62%) by the treatment of 1,3-dichloro-2-germatrisilane (**C**) with lithium in the presence of biphenyl. Compound **2**

* Corresponding authors.

Table 1
Selected bond distances (Å) for **1** (estimated standard deviations in parentheses)

Ge(1)–Si(1)	2.480(3)	Si(1)–Si(2)	2.418(5)	Si(2)–Ge(1)	2.458(4)
Ge(1)–C(1)	1.957(13)	Ge(1)–C(5)	1.971(12)	Si(1)–C(9)	1.899(13)
Si(1)–C(14)	1.882(14)	Si(2)–C(19)	1.872(13)	Si(2)–C(24)	1.912(13)
Si(3)–C(1)	1.870(15)	Si(4)–C(5)	1.862(11)		

was prepared by the reaction of **C** with sodium hydroxide in ethanol (45%).

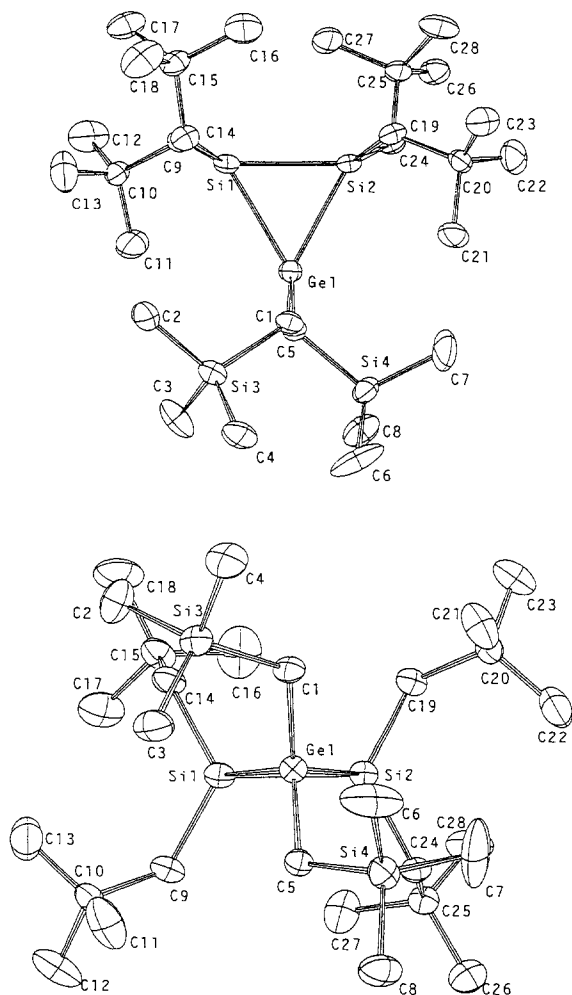
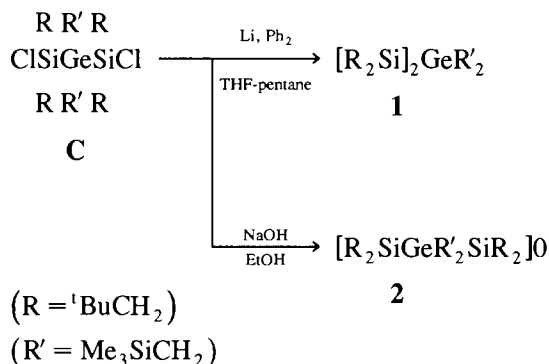


Fig. 1. Molecular structure of **1**.

The compounds **1** and **2**, which are indefinitely air stable like the four-membered germatrisilacyclobutanes **A** and **B**, were identified by the usual manner (NMR, IR and mass spectral data, as well as elemental analysis).

2.2. Molecular structures of **1** and **2**

The molecular structures of **1** and **2**, determined by X-ray crystal analysis, are shown in Figs. 1 and 2 respectively.

The four-membered GeSi₂O ring of **2** has an almost planar structure similar to the Si₃O ring of trisilaoxetane ((^tBuCH₂)₂Si)₃O (**D**) [5], in contrast with the folded structures of Si₃Ge ring [6] in **A** and **B**, and the Si₄ ring in [R₂Si]₄ (R = ^tPr [4f] or ^tBuCH₂ [8]). The crystallographic units of the both compounds comprise four molecules. The selected bond distances and angles for **1** are listed in Tables 1 and 2, and for **2** in Tables 3 and 4 respectively. Table 5 summarizes comparisons of bond distances for the two with the related compounds.

The Si–Si bond distance (2.418 Å) of **1** (Table 1) was found to be considerably longer than that of [(Me₃Si)₂Si]₂Ge(SiMe₃)₂ (2.377 Å) [1] consisting of the same ring system as **1**. In addition, this longer distance than that of the corresponding cyclotrisilane [(^tBuCH₂)₂Si]₃ (**E**) (2.399 Å) [4a] falls in the middle of the range of reported values for the other trisilacycles (2.34–2.511 Å) (Table 5) [9–13]. The Si–Ge bonds (2.458 and 2.480 Å; average, 2.469 Å) are considerably longer than those of [(Me₃Si)₂Si]₂Ge(SiMe₃)₂ (2.391 Å) [1], [H₂Si]₂GeH₂ (2.399 Å) [3], [H₂Ge]₂SiH₂ (2.402 Å) [3] and the related linear compounds (2.384–2.440 Å, entries 16–18 of Table 5) [14–16], except that of [Mes₂Ge]₂SiMes₂ (2.508 Å) [2b] having bulky groups. As shown above, the two bond distances of 2.418 Å for

Table 2
Selected bond angles (°) for **1** (estimated standard deviations in parentheses)

Ge(1)–Si(1)–Si(2)	60.2(1)	Si(1)–Si(2)–Ge(1)	61.1(1)
Si(2)–Ge(1)–Si(1)	58.6(1)	Si(1)–Ge(1)–C(1)	118.0(3)
Si(1)–Ge(1)–C(5)	119.6(4)	Si(2)–Ge(1)–C(1)	119.1(4)
Si(2)–Ge(1)–C(5)	117.9(4)	Si(2)–Si(1)–C(9)	118.2(5)
Si(2)–Si(1)–C(14)	115.3(5)	Ge(1)–Si(1)–C(9)	118.7(4)
Ge(1)–Si(1)–C(14)	114.2(4)	Si(1)–Si(2)–C(19)	116.9(4)
Si(1)–Si(2)–C(24)	116.4(4)	Ge(1)–Si(2)–C(19)	117.2(5)
Ge(1)–Si(2)–C(24)	115.5(4)	C(1)–Ge(1)–C(5)	113.3(5)
C(9)–Si(1)–C(14)	117.6(6)	C(19)–Si(2)–C(24)	117.6(6)

Table 3
Selected bond distances (Å) for **2** (estimated standard deviations in parentheses)

Si(1)–Ge(1)	2.395(4)	Si(2)–Ge(1)	2.360(4)	Si(1)–O(1)	1.719(10)
Si(2)–O(1)	1.666(10)	Ge(1)–C(1)	2.058(13)	Ge(1)–C(5)	1.974(13)
Si(1)–C(9)	1.865(14)	Si(1)–C(14)	1.904(15)	Si(2)–C(19)	1.899(14)
Si(2)–C(24)	1.938(13)				

Si–Si and 2.469 Å for Si–Ge in **1** are noticeably longer than the normal bond distances (Si–Si, 2.34 Å; Si–Ge, 2.39 Å) calculated using the covalent radii of Si and Ge atoms and also those (Si–Si, 2.393 Å; Si–Ge, 2.444 Å) of the tetracycle compound [(^tBuCH₂)₂Si]₃Ge(CH₂–

SiMe₃)₂ (**A**) [6] respectively. Thus the bond elongation in the ring system of **1** probably reflects the result of the combination of steric repulsions between the bulky substituents and ring strain (inner angles, 58.6; 60.2 and 61.1°).

Table 4
Selected bond angles and torsion angles (°) for **2** (estimated standard deviations in parentheses)

<i>Bond angles</i>					
Si(1)–Ge(1)–Si(2)	70.1(1)	Ge(1)–Si(1)–O(1)	89.9(3)		
Ge(1)–Si(2)–O(1)	92.4(4)	Si(1)–O(1)–Si(2)	107.6(5)		
Si(1)–Ge(1)–C(1)	116.1(4)	Si(1)–Ge(1)–C(5)	120.8(4)		
Si(2)–Ge(1)–C(1)	115.6(4)	Si(2)–Ge(1)–C(5)	120.4(4)		
Ge(1)–Si(1)–C(9)	115.9(4)	Ge(1)–Si(1)–C(14)	119.2(5)		
O(1)–Si(1)–C(9)	107.8(5)	O(1)–Si(1)–C(14)	100.8(6)		
Ge(1)–Si(2)–C(19)	117.6(5)	Ge(1)–Si(2)–C(24)	118.6(5)		
O(1)–Si(2)–C(19)	105.4(6)	O(1)–Si(2)–C(24)	104.9(6)		
C(1)–Ge(1)–C(5)	109.4(6)	C(9)–Si(1)–C(14)	116.9(7)		
C(19)–Si(2)–C(24)	110.3(6)				
<i>Torsion angles</i>					
Ge(1)–Si(1)–O(1)–Si(2)	1.6(5)	Ge(1)–Si(2)–O(1)–Si(1)	–1.6(5)		
Si(1)–Ge(1)–Si(2)–O(1)	1.2(3)	O(1)–Si(1)–Ge(1)–Si(2)	–1.1(3)		
C(1)–Ge(1)–Si(1)–C(9)	–0.9(7)	C(1)–Ge(1)–Si(2)–C(24)	3.0(7)		
C(5)–Ge(1)–Si(1)–C(14)	10.8(7)	C(5)–Ge(1)–Si(2)–C(19)	–4.8(7)		

Table 5
Comparisons of bond distances (average values) for **1**, **2** and the related compounds

Entry	Compound	Bond distance (Å)		Reference
		Si–Si	Si–Ge	
1	[(Dmp) ₂ Si] ₃ ^a	2.414	—	[9]
2	<i>cis,cis</i> -[Mes(^t Bu)Si] ₃ ^b	2.428	—	[10]
3	<i>cis,trans</i> -[Mes(^t Bu)Si] ₃ ^b	2.416	—	[10]
4	[^t Bu ₂ Si] ₃	2.511	—	[11]
5	<i>cis,trans</i> -[c-C ₆ H ₁₁ (^t Bu)Si] ₃	2.434	—	[12]
6	[Mes ₂ Ge] ₂ SiMes ₂ ^b	2.508	2.508	[2b]
7	[(Me ₃ Si) ₂ Si] ₂ Ge(SiMe ₃) ₂	2.377	2.391	[1]
8	[R ₂ Si] ₃ ^c (E)	2.391	—	[4a]
9	[R ₂ Si] ₂ GeR' ₂ ^c (I)	2.418	2.469	This work
10	[R ₂ SiGeR' ₂ SiR' ₂] ₂ O ^c (2)	—	2.378	This work
11	[R ₂ Si] ₃ O ^c (D)	2.433	—	[5]
12	[H ₂ Si] ₃	2.34	—	[13]
13	[H ₂ Si] ₂ GeH ₂	2.336	2.399	[3]
14	[H ₂ Ge] ₂ SiH ₂	—	2.402	[3]
15	[R ₂ Si] ₃ GeR' ₂ ^c (A)	2.393	2.444	[6]
16	Me ₃ Si–GePh ₃	—	2.384	[14]
17	Ph ₃ Si–GeMe ₃	—	2.394	[15]
18	Et ₃ Si–GeHMesGeMe ₃ ^b	—	2.440	[16]

^a Dmp = 2,6-dimethylphenyl.

^b Mes = 2,4,6-trimethylphenyl.

^c R = CH₂^tBu; R' = CH₂SiMe₃.

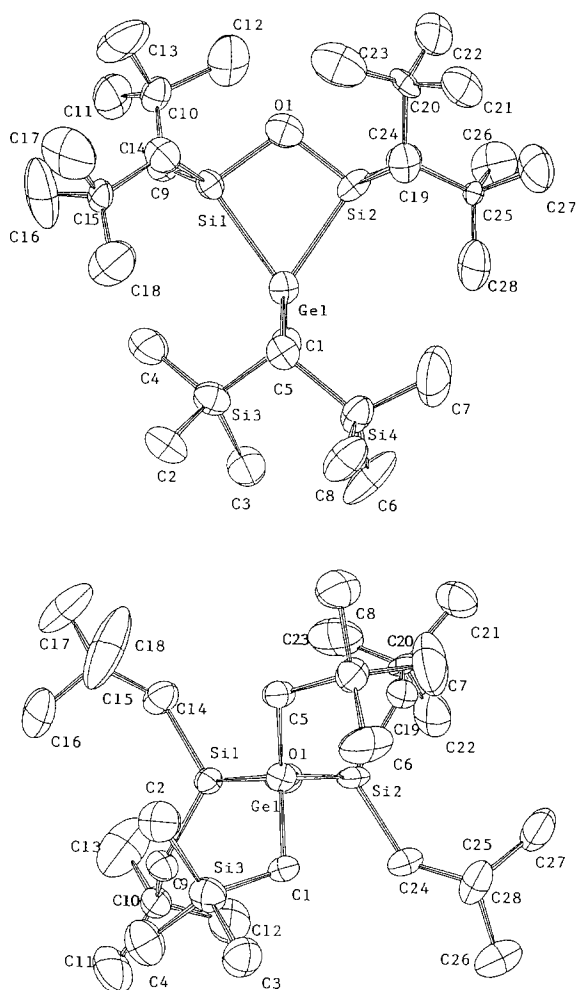


Fig. 2. Molecular structure of **2**.

Interestingly, the GeSi_2O ring of **2**, contrary to the trisilaoxetane (**D**) [5], was found to be somewhat deformed as seen from Fig. 2 with the following values: bond distances, $\text{Si}(1)\text{--Ge}$, 2.395 Å, $\text{Si}(2)\text{--Ge}$, 2.360 Å, $\text{Si}(1)\text{--O}$, 1.719 Å, and $\text{Si}(2)\text{--O}$, 1.666 Å (Table 3); ring inner angles, $\text{O--Si}(1)\text{--Ge}$, 89.9°, $\text{O--Si}(2)\text{--Ge}$, 92.4°, $\text{Si}(1)\text{--O--Si}(2)$, 107.6°, and $\text{Si}(2)\text{--Ge--Si}(1)$, 70.1° (Table 4); ring external angles, $\text{C}(9)\text{--Si}(1)\text{--C}(14)$, 116.9°, $\text{C}(1)\text{--Ge--C}(5)$, 109.4° and $\text{C}(24)\text{--Si}(2)\text{--C}(19)$, 110.3° (Table 4). The average Si--Ge bond (2.378 Å) is shorter than those of the calculated bond (2.39 Å; see above) and the other related compounds (2.384–2.508 Å) (Table 5), and also the average Si--Si bond (2.433 Å) for the corresponding trisilaoxetane **D** [5]. On the contrary, the average Si--O bond (1.693 Å) of **2** is longer than the normal bonds (average, 1.64 Å) found for a number of siloxane systems [17] and those of the corresponding trisilaoxetane **D** (1.655 Å) [5] and $[\text{H}_2\text{Si}]_3\text{O}$ (1.661 Å) [18]. The ring deformation of **2**, which is highly strained, obviously comes from the unbalanced bond length of the two total distances of the Ge--Si--O bondings, and their inner and external angle differences around the

ring metals. A noticeable fact concerning the deformation can be observed when the relationships between the external angles including the α -carbon atoms attached to the ring metals and the M--M distances of **2** and **D** are considered. For Si_3O (**D**) [5], the external angles and Si--Si distances are known to be as follows: $\text{C}(1)\text{--Si}(1)\text{--C}(2)$, 115.5°, $\text{C}(3)\text{--Si}(2)\text{--C}(4)$, 117.3°, and $\text{C}(5)\text{--Si}(3)\text{--C}(6)$, 115.0°, and $\text{Si}(1)\text{--Si}(2)$, 2.445 Å, and $\text{Si}(2)\text{--Si}(3)$, 2.421 Å respectively. Thus, in particular, the external angle (109.4°) at the Ge atom of **2** as shown above is fairly small compared with the value (117.3°) at the $\text{Si}(2)$ atom of **D**, which corresponds to the Ge atom in **2**, and a similar trend is found in the average M--M distances for the two compounds, i.e. Si--Ge , 2.378 Å, for **2** and Si--Si , 2.433 Å, for **D**. From these observations it is reasonable to consider that the bond shortening and angle decrease of GeSi_2O (**2**) relative to Si_3O (**D**) probably result in decreasing the steric repulsions between the substituents on the ring metals and releasing the ring strain as much as possible. Consequently, it clearly shows that the ring shape associated with the steric repulsions between the bulky substituents on the ring metals is closely related to the features mentioned above with respect to the ring bond distances and angles, as well as those of the external bondings. However, the reason why the GeSi_2O ring deformation occurs in the crystals to some extent in such a manner remains inexplicable at present.

Finally, it is quite interesting to note some selected angles of **1** and **2**. Thus the endocyclic Si--Ge--Si angles of **1** and **2** are 58.6° and 70.1° respectively, the latter of which is only slightly larger than the corresponding angle, Si--Si--Si (68.2°), for trisilaoxetane **D** [5]. The two angles indicated for **1** and **2** equally show that the GeSi_2 and GeSi_2O rings apparently contain large strains analogous to the corresponding cyclotrisilane **E** [4e] and trisilaoxetane **D** [5] respectively. The Si--O--Si inner angle of **2** is 107.6°, being smaller than those for the trisilaoxetane (111.1°) [5] and $[\text{H}_2\text{Si}]_3\text{O}$ (112.1°) [18],

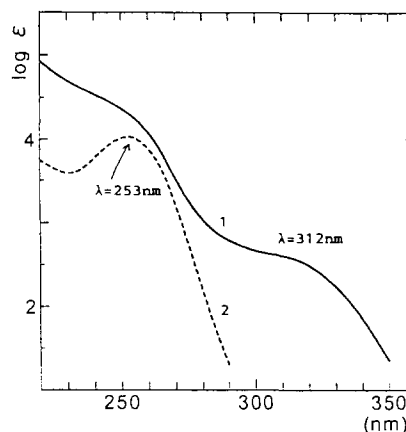


Fig. 3. UV spectra for **1** (—) and **2** (----).

and larger than those (86.2–91.3°) for cyclo-1,3-dioxanes [19]. The almost planar GeSi_2O ring of **2** was confirmed by the facts that the dihedral angle between the two planes Ge-Si(1)-O and Ge-Si(2)-O is only 1.9° and also the torsion angle for Si(2)-Ge-Si(1)-O is 1.1° (Table 4) (see also Fig. 2).

2.3. UV spectra of **1** and **2**, and ring strain energy of **1**

The longest-wavelength absorption maxima and the extinction coefficients of **1** ($\lambda_{\text{max}} = 312 \text{ nm}$ (sh), $\log \epsilon = 2.60$) and **2** ($\lambda_{\text{max}} = 253 \text{ nm}$, $\log \epsilon = 4.09$), shown in Fig. 3, are very close to those for the corresponding cyclotrisilane [$(^t\text{BuCH}_2)_2\text{Si}$] $_3$ (**E**) ($\lambda_{\text{max}} = 310 \text{ nm}$, $\log \epsilon = 2.52$) [4b], and trisilaoxetane [$(^t\text{BuCH}_2)_2\text{Si}$] $_3\text{O}$ (**D**) ($\lambda_{\text{max}} = 250 \text{ nm}$, $\log \epsilon = 4.06$) [5] respectively. The absorption maximum of **1** falls in the region of the values reported for peralkylcyclotrisilanes ($\lambda_{\text{max}} = 310\text{--}335 \text{ nm}$) [4g,20], except for the case of [$^t\text{Bu}_2\text{Si}$] $_3$ which shows its unusually long absorption maximum (390 nm) [11]. The hypsochromic shift of **2** with an increased extinction coefficient compared with **1** parallels with the cases of [Me_2Si] $_n\text{X}$ ($n = 5, 6$; $\text{X} = \text{O}$ [21], S[21] or NMe [22]) rather than [Me_2Si] $_n$ ($n = 5, 6$) [23].

Previously, we found that the ring strain energies of the peralkylcyclopolysilanes can be estimated as the differences between the transition energies of the two series (linear and cyclic) of polysilanes of the same silicon numbers ($\Delta(\Delta E) = \Delta E(\text{linear}) - \Delta E(\text{cyclic})$), by using their longest absorption bands of [R_2Si] $_n$ and $\text{Me}(\text{Me}_2\text{Si})_n\text{Me}$, where $n = 3\text{--}6$ respectively [4e]. Similarly, with the aid of the longest absorption bands of **1** ($\lambda_{\text{max}} = 312 \text{ nm}$) and the corresponding linear compound $\text{HR}_2\text{SiGeR}'_2\text{SiR}_2\text{H}$ (**F**) ($\text{R} = ^t\text{BuCH}_2$; $\text{R}' = \text{Me}_3\text{SiCH}_2$) ($\lambda_{\text{max}} = 223 \text{ nm}$; see Section 3), the ring strain energy of **1** could be equally evaluated to be 36.6 kcal mol $^{-1}$. Thus the value for **1** determined on the

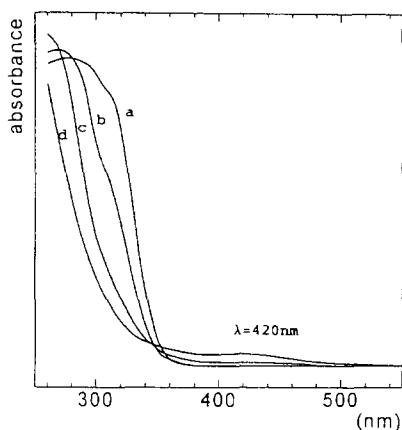


Fig. 4. Reaction profile for the photolysis of **1** in cyclohexane at room temperature: curve a, before irradiation; curve b, after irradiation for 30 min; curve c, after irradiation for 60 min; curve d, after irradiation for 90 min.

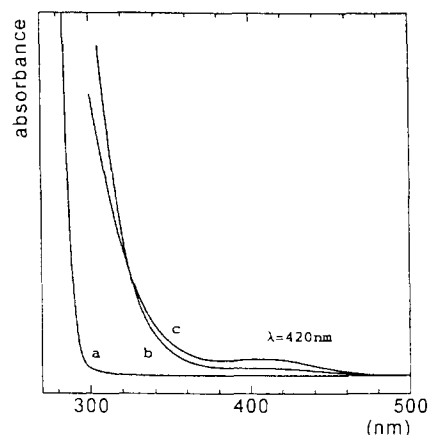


Fig. 5. Reaction profile for the photolysis of **2** in cyclohexane at room temperature: curve a, before irradiation; curve b, after irradiation for 40 min; curve c, after irradiation for 50 min.

experimental bases shows good agreement with the calculated value of 35.6 or 37.8 kcal mol $^{-1}$ for the model compound [H_2Si] $_2\text{GeH}_2$ obtained theoretically [3]. It is worthwhile to note that the above value is also very close to that of the trisilacycle Si_3 , 41 kcal mol $^{-1}$, which was experimentally determined previously [4e].

2.4. Photolysis of **1** and **2**

The photolysis was done by irradiating ($\lambda = 254 \text{ nm}$) a cyclohexane or 3-methylpentane solution of the compounds placed in a sealed tube connected with a UV-monitoring cell, and the progress of the reaction was monitored by the spectral changes during the irradiation.

First, we investigated the photolysis of **1** at room temperature. A solution of **1** (12 mg) in cyclohexane (3 ml) showed the spectral changes given in Fig. 4. Thus the solution became pale yellow in color after about 60 min, at which time the absorption band of **1** at $\lambda = 312 \text{ nm}$ almost disappeared and instead a new weak broad band at 420 nm began to appear. On further irradiation, the band at 420 nm grew and attained its maximum intensity after 90 min and began to decrease after 120 min. In separate experiments, it was observed that the band at 420 nm remained slightly after standing for 3 days in the dark but disappeared rapidly when air (O_2) was introduced into the system. In the experiments using **2**, a similar band at 420 nm was also observed by a shorter time of irradiation and began to decrease after 60 min, as shown in Fig. 5. From the above results and analogous observations to the photolyses of trisilagermacyclobutanes **A** and **B** [7], the band at 420 nm [24] may be attributable to tetrakis(trimethylsilylmethyl)digermyne ($(\text{Me}_3\text{SiCH}_2)_2\text{Ge} = \text{Ge}(\text{CH}_2\text{SiMe}_3)_2$ (**5**)) [7], which was formed via dimerization of bis(trimethylsilylmethyl)germylene ($(\text{Me}_3\text{SiCH}_2)_2\text{Ge}$ (**4**)) [7]. The other product in the photolysis of **1** at room temperature

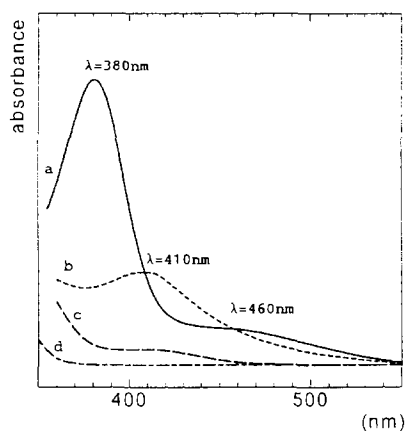


Fig. 6. UV spectra of **1** in 3-MP: curve a, —, after irradiation for 10 h at 77 K; curve b, ----, after annealing of the matrix; curve c, — · —, after complete melting of the matrix and on standing at room temperature for 1.5 h; curve d, - - -, after 10 h at room temperature.

is tetraeopentylidisilene (**3**) which should exhibit an absorption band at $\lambda = 400$ nm [4b], but this band was unable to be distinguished from the band due to the digermene **5** because of overlapping (Fig. 4). Similarly, tetraeopentylidisilaoxirane (**12**) [5] is another product from **2** after the extrusion of the germylene **4**, the details of which will be described later.

Second, in order to confirm the spectral behavior at the early stage of the reaction, the photolyses of the compounds at 77 K were carried out. Thus irradiation of **1** and **2** (12 mg) in 3-methylpentane (3 ml) for 8–10 h at 77 K produced a yellow glass, showing two absorption bands at $\lambda = 380$ and 460 nm for **1** (10 h) (Fig. 6), and at $\lambda = 318$ and 445 nm for **2** (8 h) (Fig. 7) respectively. On warming and then recooling to 77 K (annealing), the two bands from **1** disappeared and instead a relatively strong new broad band at 410 nm appeared and slowly disappeared on standing in the dark at room temperature (Fig. 6). On the contrary, the band at 445 nm from **2** also disappeared via a similar anneal to that mentioned above and then a new band at $\lambda = 398$ nm appeared. On further annealing, the two bands at 318 and 398 nm changed to a band at $\lambda = 415$ nm (Fig. 7).

The band at 460 nm from **1** at a low temperature is likely to be due to the germylene **4** [7]. Similarly, the band at 445 nm derived from **2** in the low temperature experiment may also be due to the germylene **4**, since it has previously been reported that identical germylenes arising from different precursors sometimes show different absorption maxima [25] and this is probably the case. The bands at 410–415 nm observed via the annealing of the matrices after irradiation of **1** and **2** are attributable to the same digermene **5**.

The band at $\lambda = 318$ nm at 77 K from **2** (Fig. 7) may be due to tetraeopentylidisilaoxirane (**12**) [5]. In gen-

eral, silylenes [26] and germylenes [27] have been known to form the complexes of the type $R_2M: \leftarrow B$, in the presence of Lewis bases (B) such as R_2O , R_3N and R_2S , and these complexes are known to exhibit absorption bands with larger optical densities in a shorter-wavelength region than free silylenes or germylenes do. Thus the transient band at $\lambda = 398$ nm arising from **2** via annealing of the matrix (Fig. 7) may be attributable to the germylene–disilaoxirane complex, $R'_2Ge: \leftarrow O[SiR'_2]_2$ ($R = {}^tBuCH_2$; $R' = Me_3SiCH_2$), followed by the formation of the digermene **5** on further annealing the matrix. Regarding the strong absorption band appearing at $\lambda = 380$ nm from **1** at 77 K, presumably this is not attributable to the disilene **3** since the latter is not known to exhibit its absorption band near $\lambda = 380$ nm. Further, the disilene absorption band, even if it exists in this case, falls in the range between the former strong peak and the germylene peak ($\lambda = 460$ nm), from which the disilene band could not be distinguished (Fig. 6). Consequently, the origin of the band at $\lambda_{max} = 380$ nm is not clear at present, but it may come from some kinds of Si and/or Ge radical [7,28], because of the detection of complex (mixed) electron spin resonance (ESR) signals attributable to such species. It is worthwhile to note that, in the similar photolysis of $[({}^tBuCH_2)_2Si]_3$ (**E**) at 77 K, strong ESR signals due to Si radicals (mixed) are also observable [29].

As mentioned above, the appearance of the relatively strong absorption bands in the 410–415 nm region assignable to the digermene **5**, after annealing (Fig. 6 for **1** and Fig. 7 for **2**) can be explained in terms of the formation of the digermene **5** which has its larger molar extinction coefficient [30] than that of the germylene **4**. With respect to the molar extinction coefficients, it has recently been shown that the values of digermenes are much larger than those of the germylenes [20,31]. Thus

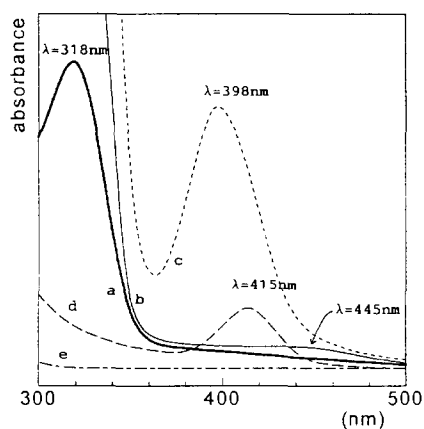
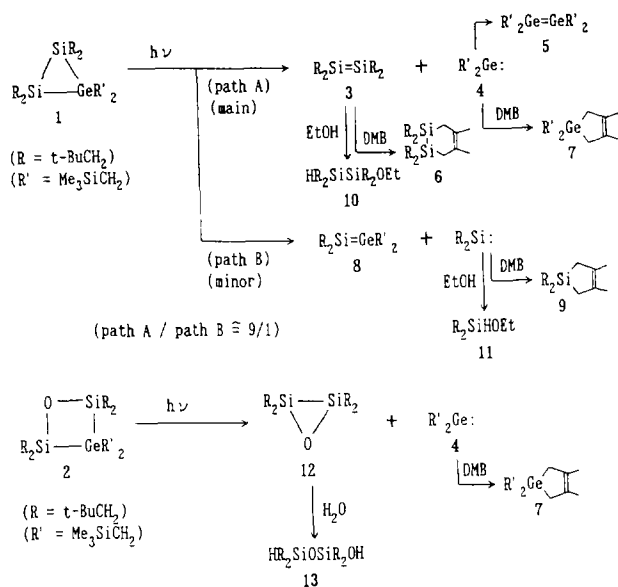


Fig. 7. UV spectra of **2** in 3-MP: curve a, —, after irradiation for 0.5 h at 77 K; curve b, ----, after irradiation for 8 h at 77 K; curve c, — · —, after annealing of the matrix; curve d, - - -, after further annealing of the matrix; curve e, - - -, after complete melting up to room temperature.

Scheme 1. Possible pathways from **1** and **2** to the products.

the qualitative observations mentioned above strongly suggest that the photolysis of **1** and **2** gave rise to the transient species, disilene **3** and disilaoxirane **12** respectively, with extrusion of germylene **4**, as shown in Scheme 1.

To obtain further insight into the photochemical processes actually occurring, trapping experiments of the reactive intermediates such as disilene **3** and germylene **4** with 2,3-dimethylbutadiene (DMB) or ethanol were carried out at room temperature. The products **7** [7] and **9** [7] were isolated by means of preparative gas–liquid chromatography (GLC) and identified by comparisons of the GLC retention times and mass spectroscopy (MS) fragmentation patterns with those of the authentic samples prepared by alternative methods. The products **6**, **10**, **11** and **13** were similarly isolated and characterized by the usual manner (see Section 3). Thus irradiation (1 h) of **1** (conversion, 100%) in cyclohexane containing a large excess of the butadiene afforded the expected disilene trapping product, 1,2-disilacyclohex-4-ene (**6**) (48%), and the germylene trapping product, 1-germacyclopent-3-ene (**7**) (56%), together with a small amount of silylene trapping product, 1-silacyclopent-3-ene (**9**) (4%). Similarly, as shown in Scheme 1, irradiation (20 min) of **1** (conversion, 100%) in the presence of ethanol as a trapping agent gave the disilene trapping product, 1-ethoxy-1,1,2,2-tetraneopentyl-disilane (**10**) (73%) [4b], and silylene trapping product, dineopentylethoxysilane (**11**) (6%) [4b]. Compounds **9** and **11** may be explained in terms of the formations of silylene from **1** (path B). The experiment using **2** in the presence of the butadiene (20 min; conversion, 56%) produced the germylene trapping product **7** (29%) and silanol **13** (26%) [32], without the formation of silylene trapping product **9**.

In conclusion, from the foregoing observations and the results in the trapping experiments, it was found that

peralkyldisilagermirane (**1**) and germadisilaoxetane (**2**) photochemically decompose mainly into disilene (**3**) and disilaoxirane (**12**) respectively, with extrusion of germylene (**4**).

3. Experimental section

All the reactions were carried out using a dry flask under an atmosphere of inert gas (N₂ or Ar). IR spectra were recorded with a Hitachi EPI-G3 spectrometer. ¹H and ¹³C NMR spectra were recorded using a Varian Gemini-200M spectrometer in CDCl₃ or C₆D₆ with Me₄Si as an internal standard. ²⁹Si NMR spectra were recorded with a Hitachi 90H spectrometer. Mass spectral analyses were recorded using a JEOL DX-302 spectrometer (*I*_p = 70 eV). UV spectra were obtained using a Hitachi 200-10 spectrometer. GLC analyses were performed using an Ohkura GC-103 gas chromatograph equipped with a glass column (1 m) packed with SE-30 (10%) on Celite 545-AW (60–80 mesh). Product yields from the photolyses of **1** and **2** were determined by the GLC method, in which the thermal conductivity correction has been made using an external standard (paraffin, C₁₇H₃₆). The tetrahydrofuran (THF), ether and benzene used in the syntheses were dried over sodium wire and freshly distilled in a flask containing benzophenone-ketyl radical before use. Cyclohexane and pentane were dried over lithium aluminum hydride and freshly distilled before use. Other solvents and materials were commercially available.

3.1. Preparation of 1,1,3,3-tetraneopentyl-2,2-bis(trimethylsilylmethyl)-1,3-dichloro-1,3-disila-2-germapropane (**C**)

To a solution of 1,1,3,3-tetraneopentyl-2,2-bis(trimethylsilylmethyl)-1,3-disila-2-germapropane (HSiR₂-GeR'₂SiR₂H (R = ¹BuCH₂; R' = Me₃SiCH₂) (**F**) (3.54 g, 6.0 mmol) in benzene (50 ml) and phosphorus pentachloride (3.78 g, 13.3 mmol) was added at room temperature. After the reaction mixture became clear, the resulting solution was refluxed for 3 h and concentrated to give a semisolid. Pentane (100 ml) was added and unreacted phosphorus pentachloride was filtered off. Evaporation of the filtrate afforded a solid which was recrystallized from hot acetonitrile to give colorless crystals of **C** (yield, 2.60 g (66%); melting point (m.p.), 81–83°C (sealed capillary)). ¹H NMR (CDCl₃): δ 0.11 (s, 18H, SiCH₃), 0.22 (s, 4H, CH₂SiMe₃), 1.12 (s, 36H, C(CH₃)₃), 1.29 (s, 8H, CH₂¹Bu) ppm. ¹³C NMR (CDCl₃): δ -1.15 (CH₂SiMe₃), 2.49 (SiCH₃), 32.54 (CMe₃), 33.14 (C(CH₃)₃), 35.60 (CH₂¹Bu) ppm. IR (KBr pellet) ν(Si–Cl) 480 cm⁻¹. MS: *m/e* (relative intensity) 643 (4, [M – Me]⁺), 587 (7, [M – CH₂¹Bu]⁺), 453 (100, [M – (ClSi(CH₂¹Bu)₂]⁺).

The 1,3-dihydrotrimetallane (**F**) mentioned above was prepared with an 82% yield by the reaction of di-neopentylchlorosilane ($^1\text{BuCH}_2)_2\text{Si}(\text{H})\text{Cl}$ (**G**) and bis(trimethylsilylmethyl)germanium dichloride [**7b**] with lithium in THF at 0°C (m.p., 74–76°C (sealed capillary)). ^1H NMR (C_6D_6): δ 0.25 (s, 18H, SiCH_3), 0.33 (s, 4H, CH_2SiMe_3), 1.14 (s, 36H, $\text{C}(\text{CH}_3)_3$), 1.15 (double ABq, $J_{\text{CH}_2-\text{SiH}} = 3.7$ Hz, $J_{\text{AB}} = 14.7$ Hz, $\Delta\nu_{\text{AB}} = 43$ Hz, 8H, CH_2^1Bu), 4.52 (quintet, $J = 3.6$ Hz, 2H, SiH) ppm. ^{13}C NMR (CDCl_3): δ -1.78 (CH_2SiMe_3), 2.27 (SiCH_3), 29.69 (CH_2^1Bu), 31.07 (CMe_3), 32.40 ($\text{C}(\text{CH}_3)_3$) ppm. UV (cyclohexane): $\lambda_{\text{max}} = 223$ nm (sh) ($\epsilon = 7100$ mol $^{-1}$ dm 3 cm $^{-1}$). IR (KBr pellet) $\nu(\text{Si-H})$ 2116 cm $^{-1}$. MS: m/e (relative intensity) 590 (2, M^+), 575 (3, $[\text{M} - \text{CH}_3]^+$), 519 (2, $[\text{M} - \text{CH}_2^1\text{Bu}]^+$), 419 (100, $[\text{M} - (^1\text{BuCH}_2)_2\text{SiH}]^+$). Anal. Found: C, 57.01; H, 11.83. $\text{C}_{28}\text{H}_{68}\text{Si}_4\text{Ge}$ calc.: C, 57.02; H, 11.62%.

The chlorosilane (**G**) described above was synthesized with a 63% yield by the reaction of trichlorosilane with neopentyllithium, prepared from neopentylchloride [33] and lithium in petroleum ether (boiling point, 85–87°C (36 Torr)). ^1H NMR (CDCl_3): δ 0.98 (br s, 22H, $\text{CH}_2\text{C}(\text{CH}_3)_3$), 4.95 (br s, 1H, SiH) ppm. ^{13}C NMR (CDCl_3): δ 34.27 (CH_2^1Bu), 32.47 ($\text{C}(\text{CH}_3)_3$), 30.78 (CMe_3) ppm. IR (neat) $\nu(\text{Si-H})$ 2164 cm $^{-1}$.

3.2. Preparation of 1

A solution of **C** (0.66 g, 1.0 mmol) in THF: pentane (12 ml; 1:1 by volume) was added at a stretch to the

green-colored mixture of lithium (0.084 g, 12.1 mmol) and biphenyl (0.037 g, 0.24 mmol) in THF: pentane (6 ml; 1:1 by volume) at 0°C. After 30 min stirring at 0°C, cyclohexane was added to the reaction mixture and the mixture then filtered. The resulting solution was concentrated to give a solid product which was recrystallized from EtOH–pentane at -15°C, affording air-stable and colorless crystals of **1** (yield, 0.36 g (62%); m.p., 136–137°C (sealed capillary)), ^1H NMR (C_6D_6): δ 0.25 (s, 18H, SiCH_3), 0.33 (s, 4H, CH_2SiMe_3), 1.19 (s, 36H, $\text{C}(\text{CH}_3)_3$), 1.28 (br s, 8H, CH_2^1Bu) ppm. ^{13}C NMR (C_6D_6): δ -0.42 (CH_2SiMe_3), 1.60 (SiCH_3), 30.33 (CH_2^1Bu), 32.06 (CMe_3), 33.72 ($\text{C}(\text{CH}_3)_3$) ppm. ^{29}Si NMR (C_6D_6): δ -69.34 (ring), 2.34 (SiMe) ppm. UV (cyclohexane): $\lambda_{\text{max}} = 312$ nm (sh) ($\epsilon = 400$ mol $^{-1}$ dm 3 cm $^{-1}$). IR (KBr pellet); ν 2948 (s), 2898 (s), 2860 (s), 2708 (w), 1474 (m), 1396 (m), 1384 (m), 1362 (m), 1304 (w), 1246 (s), 1228 (s), 1152 (m), 1116 (m), 1034 (s), 1020 (m), 1010 (m), 978 (m), 934 (w), 854 (s), 830 (s), 784 (s), 770 (s), 720 (s), 708 (s), 694 (s), 684 (s), 618 (m), 590 (w), 548 (m), 478 (w), 402 (w), 358 (w), 336 (w) cm $^{-1}$. MS: m/e (relative intensity) 588 (20, M^+), 573 (3, $[\text{M} - \text{Me}]^+$), 515 (4, $[\text{M} - \text{SiMe}_3]^+$), 459 (7, $[\text{M} - \text{SiMe}_3 - \text{C}_4\text{H}_8]^+$), 442 (20), 144 (100). Anal. Found: C, 56.98; H, 11.14. $\text{C}_{28}\text{H}_{66}\text{Si}_4\text{Ge}$ calc.: C, 57.22; H, 11.32%.

3.3. Preparation of 2

A solution of sodium hydroxide (0.12 g, 3.0 mmol) in ethanol (5 ml) was added dropwise to **C** (0.65 g, 0.98

Table 6

Crystallographic data for $[(^1\text{BuCH}_2)_2\text{Si}]_2\text{Ge}(\text{CH}_2\text{SiMe}_3)_2$ (**1**) and $[(^1\text{BuCH}_2)_2\text{SiGe}(\text{CH}_2\text{SiMe}_3)_2\text{Si}(\text{CH}_2^1\text{Bu})_2]\text{O}$ (**2**)

	1	2
Formula	$\text{C}_{28}\text{H}_{66}\text{Si}_4\text{Ge}$	$\text{C}_{28}\text{H}_{66}\text{OSi}_4\text{Ge}$
Formula weight	587.78	603.78
Crystal size (mm)	0.1 × 0.6 × 0.1	0.3 × 0.3 × 0.2
Crystal system	Monoclinic	Orthorhombic
Space group	$P2_1/n$	$P2_12_12_1$
a (Å)	12.251(3)	11.770(2)
b (Å)	15.766(3)	16.215(1)
c (Å)	20.863(5)	20.613(3)
β (°)	103.31(1)	
V (Å 3)	3921.5(1.5)	3934.0(9)
Z	4	4
D_{calcd} (g cm $^{-3}$)	0.9954	1.0191
μ (Cu K α), cm $^{-1}$	23.49	23.7
Scan mode	ω -2 θ	ω -2 θ
Scan speed	4.12–1.03	4.12–1.03
Scan range	4–120	4–120
Number of reflections		
Collected	6238	3305
Observed ($ F_o \geq 3\sigma F_o $)	2407	2520
Transmission factor; minimum; maximum	0.9023; 0.9993	0.8584; 0.9943
R (R_w)	0.0822 (0.0981)	0.0825 (0.0776)
Differential Fourier map (electrons Å $^{-3}$)	Maximum, 0.997; minimum, -0.432	Maximum, 1.2; minimum, -0.8

$R = \sum ||F_o| - |F_c|| / \sum |F_o|$; $R_w = [\sum w(|F_o| - |F_c|)^2 / \sum wF_o^2]^{1/2}$;
 $w = 1/0.01161|F_o|^2 - 0.4484|F_o| + 10.307$ and $1/\sigma^2|F_o|$ for **1** and **2** respectively.

mmol) in THF (10 ml). After stirring for 20 min, cyclohexane was added to the reaction mixture and the mixture then filtered. The resulting solution was concentrated to give a solid product which was recrystallized from EtOH, affording air-stable and colorless crystals of **2** (yield, 0.27 g (45%); m.p., 124–130°C (sealed capillary)). ¹H NMR (CDCl₃): δ 0.05 (s, 18H, SiCH₃), 0.28 (s, 4H, CH₂SiMe₃), 1.05 (s, 36H, C(CH₃)₃), 1.09 (ABq, *J*_{AB} = 14.7 Hz, Δ*ν*_{AB} = 37 Hz, 8H, CH₂¹Bu) ppm. ¹³C NMR (CDCl₃): δ -0.09 (CH₂SiMe₃), 1.87 (SiCH₃), 31.37 (CMe₃), 33.50 (C(CH₃)₃), 37.22 (CH₂¹Bu) ppm. ²⁹Si NMR (CDCl₃): δ 7.10 (SiMe), 40.68 (ring) ppm. UV (cyclohexane): λ_{max} = 253 nm (ε = 12 600 mol⁻¹ dm³ cm⁻¹). IR (KBr pellet): ν 2956 (s), 2890 (s), 1476 (s), 1401 (m), 1386 (m), 1365 (s), 1248 (s), 1158 (m), 1113 (m), 1038 (s), 1017 (m), 984 (w), 936 (w), 912 (w), 858 (s, ν_{SiOSi}), 828 (s), 780 (s), 759 (s), 726 (s), 684 (m), 621 (m), 591 (w), 543 (w), 498 (w), 429 (w), 378 (w), 354 (w) cm⁻¹. MS: *m/e* (relative intensity) 604 (12, M⁺), 589 (6, [M - Me]⁺), 531 (19, [M - SiMe₃]⁺), 443 (100). Anal. Found: C, 55.42; H, 11.10. C₂₈H₆₆O₄Si₄Ge calc.: C, 55.70; H, 11.02%.

3.4. X-ray crystal analyses of **1** and **2**

Crystals, obtained from pentane–ethanol for **1** and ethanol for **2**, were used for the X-ray analyses. Intensity data were obtained on a Enraf–Nonius CAD-4 diffractometer equipped with graphite-monochromated Cu Kα radiation (λ = 1.5418 Å) and using the ω–2θ scan technique (2θ < 120° for **1** and **2**). The structures of both **1** and **2** were solved by direct methods using the MULTAN 78 program [34] and refined by the full-matrix least-squares method. All hydrogen atoms for **1** and **2** were located in their calculated positions. The final refinements with anisotropic temperature factors for the non-hydrogen atoms had lowered the *R* value to 0.0822 (*R*_w = 0.0981) for **1** and 0.0825 (*R*_w = 0.0776) for **2**. All the calculations were performed with UNICS III systems [35]. The molecular structures, selected bond distances and angles, and atomic coordinates for the non-hydrogen atoms are given in Fig. 1 and Tables 1, 2 and 7 for **1**, and Fig. 2 and Tables 3, 4 and 8 for **2**. The crystallographic data for **1** and **2** are summarized in Table 6.

3.5. Photolysis of **1** and **2** in cyclohexane at room temperature

In a typical experiment, **1** (12 mg, 2.0 × 10⁻⁵ mol) and cyclohexane (3 ml) were placed in a quartz tube fitted with a UV-monitoring cell. After the solution had been degassed by freeze–pump–thaw cycles, the reaction tube was sealed. The solution was irradiated with a low pressure mercury lamp (30 W) at room tempera-

Table 7

Fractional atomic coordinates and equivalent isotropic thermal parameters for **1** (estimated standard deviations in parentheses)

Atom	x	y	z	<i>B</i> _{eq} ^a (Å ²)
Ge(1)	0.3474(1)	0.2352(1)	0.2596(1)	6.36(5)
Si(1)	0.5465(2)	0.2668(2)	0.3114(2)	6.4(1)
Si(2)	0.4965(2)	0.2116(2)	0.2004(2)	6.0(1)
Si(3)	0.2334(3)	0.1438(3)	0.3719(2)	8.3(1)
Si(4)	0.1142(3)	0.3093(3)	0.1638(2)	8.9(1)
C(1)	0.2780(10)	0.1374(8)	0.2921(6)	7.1(4)
C(2)	0.3541(14)	0.1318(13)	0.4429(8)	12.4(8)
C(3)	0.1649(19)	0.2442(10)	0.3816(9)	13.5(9)
C(4)	0.1344(14)	0.0539(12)	0.3733(9)	11.8(7)
C(5)	0.2419(10)	0.3293(8)	0.2302(6)	6.6(4)
C(6)	0.0148(15)	0.2415(13)	0.1959(16)	19.4(13)
C(7)	0.1461(22)	0.2539(22)	0.0966(10)	24.3(16)
C(8)	0.0388(14)	0.4095(11)	0.1398(10)	12.8(8)
C(9)	0.5923(10)	0.3819(8)	0.3234(7)	7.8(5)
C(10)	0.5620(11)	0.4402(9)	0.3760(8)	7.7(5)
C(11)	0.4387(15)	0.4606(15)	0.3572(12)	16.3(10)
C(12)	0.6269(17)	0.5249(12)	0.3795(13)	15.8(11)
C(13)	0.5931(21)	0.4028(16)	0.4423(11)	16.2(11)
C(14)	0.6145(11)	0.1884(8)	0.3765(7)	8.0(5)
C(15)	0.7413(12)	0.1640(10)	0.3907(9)	9.1(6)
C(16)	0.7689(15)	0.1315(17)	0.3282(13)	17.5(11)
C(17)	0.8155(13)	0.2396(12)	0.4182(11)	12.8(8)
C(18)	0.7677(17)	0.0977(13)	0.4443(13)	16.2(10)
C(19)	0.5362(9)	0.0990(8)	0.1884(7)	6.9(4)
C(20)	0.4677(11)	0.0364(9)	0.1381(7)	7.4(5)
C(21)	0.3548(14)	0.0199(12)	0.1541(10)	12.9(8)
C(22)	0.4461(16)	0.0707(12)	0.0702(10)	12.6(8)
C(23)	0.5298(14)	-0.0460(11)	0.1377(10)	12.2(8)
C(24)	0.5002(9)	0.2904(8)	0.1312(6)	6.7(4)
C(25)	0.6118(11)	0.3177(10)	0.1135(7)	7.3(5)
C(26)	0.5869(12)	0.3789(11)	0.0566(9)	10.3(6)
C(27)	0.6903(13)	0.3597(14)	0.1729(9)	12.5(8)
C(28)	0.6707(14)	0.2430(11)	0.0914(11)	12.4(8)

^a Thermal parameters are given by the equivalent temperature factors.

ture, and the electronic spectra were observed at periodic intervals during the irradiation (Fig. 4). After irradiation for 1 h (pale yellow) the seal of the reaction cell was opened; thus a colorless solution, for which the electronic spectrum was measured, was obtained. Similarly, the experiment using **2** was carried out and the electronic spectra were obtained (Fig. 5).

3.6. Irradiation of **1** and **2** in 3-methylpentane at 77 K

Typically, **1** (12 mg, 2.0 × 10⁻⁵ mol) and 3-methylpentane (3 ml) were placed in a quartz cell. After the solution had been degassed by freeze–pump–thaw cycles, the sealed cell was placed into a quartz Dewar filled with liquid nitrogen. The resulting matrix was similarly irradiated through the quartz window, and the electronic spectra were taken at periodic intervals. Irradiation of the matrix for 10 h at 77 K produced a pale-yellow glass with two absorption bands at 380 and

460 nm, as shown in Fig. 6. The spectral changes via annealing are also shown in Fig. 6. Similarly, the experiment using **2** was carried out and the electronic spectra were obtained as shown in Fig. 7.

3.7. Photolysis of **1** and **2** in the presence of trapping agents (2,3-dimethylbutadiene or ethanol)

Typically, a mixture of **1** (12 mg, 2.0×10^{-5} mol), 2,3-dimethylbutadiene (70 μ l, 6.2×10^{-4} mol) and cyclohexane (3 ml) was placed in a quartz reaction cell and degassed by freeze–pump–thaw cycles, and then the cell was sealed. The solution was irradiated for 1 h at room temperature. The resulting colorless solution showed no absorption band of **1** used at 312 nm and the seal of the reaction cell was opened. After evaporation of the solvent, the products formed were isolated by preparative GLC and subjected to gas chromatography–MS analysis. Thus, by comparison with the GLC retention times and MS fragmentation patterns of the authen-

tic samples, the products were identified to be **6**, **7** and **9**. The yields of **6**, **7** and **9** were determined by the GLC techniques mentioned above to be 48, 56 and 4% respectively. The experiment in the presence of ethanol as a trapping agent was carried out (20 min; conversion, 100%) to give **10** (73%) and **11** (6%). Similarly, the experiment using **2** in the presence of 2,3-dimethylbutadiene was carried out (20 min; conversion, 56%) to give **7** (26%) and **13** (26%).

3.8. Characterizations of the products formed in the photolyses using **1** and **2**

3.8.1. 1,1,2,2-tetraneopentyl-3,4-dimethyl-1,2-disilacyclohex-4-ene (**6**).

Liquid. $^1\text{H NMR}$ (CDCl_3): δ 0.92 (s, 8H, $\text{C}_2\text{H}_2^1\text{Bu}$), 1.04 (s, 36H, $\text{C}(\text{CH}_3)_3$), 1.67 (s, 4H, $\text{C}_2\text{H}_2\text{-C=}$), 1.72 (s, 6H, $=\text{CC}_2\text{H}_5$) ppm. $^{13}\text{C NMR}$ (CDCl_3): δ 22.92 (C-C=), 24.76 ($=\text{CC}_2\text{H}_5$), 29.15 (CH_2^1Bu), 31.6 (CMe_3), 33.5 ($\text{C}(\text{CH}_3)_3$), 124.8 (C=) ppm. MS: m/e

Table 8

Fractional atomic coordinates and equivalent isotropic thermal parameters for **2** (estimated standard deviations in parentheses)

Atom	x	y	z	B_{eq}^a (\AA^2)
Ge(1)	0.1126(2)	0.2566(1)	0.7592(1)	6.30(5)
Si(1)	0.2921(3)	0.2262(2)	0.8084(2)	5.2(1)
Si(2)	0.2606(3)	0.2813(2)	0.6844(2)	5.7(1)
Si(3)	-0.0366(4)	0.3584(3)	0.8718(2)	7.8(2)
Si(4)	-0.1144(4)	0.1801(3)	0.6832(3)	8.0(2)
O(1)	0.3597(7)	0.2513(6)	0.7371(4)	7.6(3)
C(1)	0.0300(13)	0.3599(7)	0.7931(7)	6.5(5)
C(2)	-0.1085(16)	0.2638(11)	0.8952(8)	10.0(7)
C(3)	-0.1455(17)	0.4411(11)	0.8711(9)	10.1(7)
C(4)	0.0642(16)	0.3825(12)	0.9328(8)	10.3(8)
C(5)	0.0005(12)	0.1684(7)	0.7430(7)	6.4(4)
C(6)	-0.2090(20)	0.2651(11)	0.7013(12)	15.2(10)
C(7)	-0.0702(26)	0.1991(19)	0.6080(11)	18.8(15)
C(8)	-0.1901(18)	0.0847(11)	0.6733(11)	11.8(9)
C(9)	0.3409(11)	0.3001(8)	0.8719(6)	6.0(5)
C(10)	0.4616(12)	0.3332(9)	0.8800(7)	6.9(6)
C(11)	0.4728(18)	0.3875(14)	0.9389(9)	12.5(9)
C(12)	0.5004(20)	0.3817(13)	0.8200(11)	13.2(10)
C(13)	0.5450(17)	0.2576(16)	0.8835(13)	17.0(13)
C(14)	0.3374(14)	0.1142(9)	0.8182(8)	8.0(6)
C(15)	0.2841(12)	0.0545(8)	0.8669(8)	6.3(5)
C(16)	0.3072(30)	0.0832(14)	0.9309(10)	18.8(16)
C(17)	0.3502(22)	-0.0236(12)	0.8690(14)	16.4(13)
C(18)	0.1737(22)	0.0443(21)	0.8609(16)	24.1(19)
C(19)	0.2742(15)	0.2082(8)	0.6129(7)	7.5(6)
C(20)	0.3949(11)	0.1736(6)	0.5927(5)	4.9(4)
C(21)	0.3672(17)	0.1251(11)	0.5265(8)	10.0(7)
C(22)	0.4732(16)	0.2402(13)	0.5765(8)	11.3(8)
C(23)	0.4322(20)	0.1136(13)	0.6384(12)	13.8(11)
C(24)	0.2993(13)	0.3944(8)	0.6636(7)	6.8(5)
C(25)	0.2332(9)	0.4474(6)	0.6145(5)	3.8(4)
C(26)	0.2829(19)	0.5384(11)	0.6149(11)	11.7(9)
C(27)	0.2511(20)	0.4158(11)	0.5426(9)	11.3(9)
C(28)	0.1165(21)	0.4498(12)	0.6238(10)	12.2(9)

^a Thermal parameters are given by the equivalent temperature factors.

(relative intensity) 422 (70, M^+), 351 (90, $[M - CH_2^1Bu]^+$), 340 (45, $[M - C_6H_{10}]^+$), 73 (100, $SiMe_3$) ppm. Anal. Found: C, 73.90; H, 12.92. $C_{26}H_{54}Si_2$ calc.: C, 73.85; H, 12.87%.

3.8.2. 1-ethoxy-1,1,2-tetraneopentylidisilane (10).

Liquid. 1H NMR ($CDCl_3$): δ 0.7–1.2 (m, 11H, $SiCH_2$ and OCH_2CH_3), 1.01 (s, 18H, $C(CH_3)_3$), 1.04 (s, 18H, $C(CH_3)_3$), 3.67 (quartet, 2H, OCH_2CH_3), 3.90 (br s, 1H, SiH) ppm. IR (neat): ν (Si–H) 2104 cm^{-1} . MS: m/e (relative intensity) 357 (15, $[M - Et]^+$), 315 (20, $[M - CH_2^1Bu]^+$), 215 (90), 103 (100). Anal. Found: C, 66.30; H, 12.93 (see [4b]). $C_{22}H_{50}OSi_2$ calc.: C, 66.60; H, 13.04%.

3.8.3. Dineopentylethoxysilane (11).

Liquid. 1H NMR (CCl_4): δ 0.73 (m, 4H, CH_2^1Bu), 1.02 (s, 18H, $C(CH_3)_3$), 1.17 (t, 3H, OCH_2CH_3), 3.65 (quartet, 2H, OCH_2CH_3), 4.72 (quintet, 1H, Si–H) ppm. IR (neat): ν (Si–H) 2120 cm^{-1} . MS: m/e (relative intensity) 216 (5, M^+), 201 (85, $[M - Me]^+$), 145 (100). Anal. Found: C, 68.44; H, 12.96 (see [4b]). $C_{12}H_{28}OSi$ calc.: C, 68.31; H, 13.02%.

3.8.4. 1,1,3-tetraneopentyl-1-hydroxydisiloxane (13).

Liquid. 1H NMR ($CDCl_3$): δ 0.71 (s, 4H, $HOSiCH_2^1Bu$), 0.77, 0.78, 0.79 and 0.81 (4H, $HSiCH_2^1Bu$), 1.02 and 1.03 (36H, $C(CH_3)_3$), 4.97 (quintet, $J = 2.5$ Hz, 1H, Si–H) ppm. ^{13}C NMR ($CDCl_3$): δ 30.31 and 30.51 (CMe_3), 32.70 and 33.09 ($C(CH_3)_3$), 34.17 and 34.38 (CH_2^1Bu) ppm. IR (neat): ν ((Si)O–H) 3696; ν (Si–H) 2128; ν (SiOSi) 1080 cm^{-1} . MS: m/e (relative intensity) 359 (8, $[M - CH_3]^+$), 303 (100, $[M - CH_2^1Bu]^+$), 247 (30), 191 (25), 135 (90). Anal. Found: C, 64.11; H, 12.12. $C_{20}H_{46}Si_2O$ calc.: C, 64.10; H, 12.37%.

Acknowledgments

We are grateful to Toshiba Silicone Co., Ltd. and Shin-Etsu Chemical Co., Ltd. for a generous gift of chlorosilanes. We are also grateful to ASAI Germanium Research Institute for a gift of tetrachlorogermane.

References and notes

- [1] A. Heine and D. Stalke, *Angew. Chem., Int. Edn. Engl.*, **33** (1994) 113.
- [2] (a) K.M. Baines and J.A. Cook, *Organometallics*, **10** (1991) 3419; (b) K.M. Baines, J.A. Cook, N.C. Payne and J.J. Vittal, *Organometallics*, **11** (1992) 1408; (c) K.M. Baines and J.A. Cooke, *Organometallics*, **11** (1992) 3487; (d) K.M. Baines, J.A. Cook, C.E. Dixon, H.W. Liu and M.R. Netherton, *Organometallics*, **13** (1994) 631.
- [3] D.A. Horner, R.S. Grev and H.F. Schaefer III, *J. Am. Chem. Soc.*, **114** (1992) 2093.
- [4] (a) H. Watanabe, M. Kato, T. Okawa, Y. Nagai and M. Goto, *J. Organomet. Chem.*, **271** (1984) 225; (b) H. Watanabe, T. Okawa, M. Kato and Y. Nagai, *J. Chem. Soc., Chem. Commun.*, (1983) 781; (c) H. Watanabe, Y. Kougo and Y. Nagai, *J. Chem. Soc., Chem. Commun.*, (1984) 66; (d) H. Watanabe, T. Muraoka, M. Kageyama, M. Yoshizumi and Y. Nagai, *Organometallics*, **3** (1984) 141; (e) H. Watanabe, H. Shimoyama, T. Muraoka, T. Okawa, M. Kato and Y. Nagai, *Chem. Lett.*, (1986) 1057; (f) H. Watanabe, M. Kato, O. Okawa, Y. Kougo, Y. Nagai and M. Goto, *Appl. Organomet. Chem.*, **1** (1987) 157; (g) H. Watanabe, Y. Kougo, M. Kato, H. Kuwabara, H. Okawa and Y. Nagai, *Bull. Chem. Soc. Jpn.*, **57** (1984) 3019.
- [5] H. Watanabe, E. Tabei, M. Goto and Y. Nagai, *J. Chem. Soc., Chem. Commun.*, (1987) 522.
- [6] H. Suzuki, Y. Fukuda, N. Sato, H. Ohmori, M. Goto and H. Watanabe, *Chem. Lett.*, (1991) 853.
- [7] (a) H. Suzuki, K. Okabe, R. Kato, N. Sato, Y. Fukuda and H. Watanabe, *J. Chem. Soc., Chem. Commun.*, (1991) 1298; (b) H. Suzuki, K. Okabe, R. Kato, N. Sato, Y. Fukuda, H. Watanabe and M. Goto, *Organometallics*, **12** (1993) 4833.
- [8] H. Matsumoto, M. Minemura, K. Takatsuma, Y. Nagai and M. Goto, *Chem. Lett.*, (1985) 1005.
- [9] S. Masamune, Y. Hanzawa, S. Murakami, T. Bally and J.F. Blount, *J. Am. Chem. Soc.*, **104** (1982) 1150.
- [10] J.C. Dewan, S. Murakami, J.T. Snow, S. Collins and S. Masamune, *J. Chem. Soc., Chem. Commun.*, (1985) 892.
- [11] A. Schäfer, M. Weidenbruch, K. Peters and H.G. von Schnering, *Angew. Chem., Int. Edn. Engl.*, **23** (1984) 302.
- [12] K.L. Thom, S. Pohl and W. Saak, *J. Organomet. Chem.*, **329** (1987) 151.
- [13] For example: D.B. Kitchen, J.E. Jackson and L.C. Allen, *J. Am. Chem. Soc.*, **112** (1990) 3408, and references cited therein.
- [14] L. Parkanyi, C. Hernandez and K.H. Pannell, *J. Organomet. Chem.*, **301** (1986) 145.
- [15] K.H. Pannell, R.N. Kapoor, R. Raptis, L. Parkanyi and V.J. Fulop, *J. Organomet. Chem.*, **384** (1990) 41.
- [16] K.M. Baines, J.A. Cooke and J.J. Vittal, *J. Chem. Soc., Chem. Commun.*, (1992) 1484.
- [17] M.G. Voronkov, V.P. Mileshevich and U.A. Yuzhelevskii, *The Siloxane Bond*, Consultants Bureau, New York, London, 1978.
- [18] R.S. Grev and H.F. Schaefer III, *J. Am. Chem. Soc.*, **109** (1987) 6577.
- [19] (a) M.J. Michalczyk, M.J. Fink, K.J. Haller, R. West and J. Michl, *Organometallics*, **5** (1986) 531; (b) A.J. Millevolte, D.R. Powell, S.G. Johnson and R. West, *Organometallics*, **11** (1992) 1091.
- [20] For example: T. Tsumuraya, S.A. Batcheller and S. Masamune, *Angew. Chem., Int. Edn. Engl.*, **30** (1991) 902, and references cited therein.
- [21] H. Stuger, M. Eibl, E. Hengge and I. Kovacs, *J. Organomet. Chem.*, **431** (1992) 1.
- [22] T.H. Newman, R. West and R.T. Oakly, *J. Organomet. Chem.*, **197** (1980) 159.
- [23] (a) E. Carberry, R. West and G.F. Glass, *J. Am. Chem. Soc.*, **91** (1969) 5446; (b) L.F. Brough and R. West, *J. Am. Chem. Soc.*, **103** (1981) 3049.
- [24] In the results of trapping experiments (vide infra), however, the band from **1** (Fig. 4) may be due to a mixture of the digermene **5**, germasilene ($(^1BuCH_2)_2Si=Ge(CH_2SiMe_3)_2$ (**8**)) and disilene ($(^1BuCH_2)_2Si=Si(CH_2^1Bu)_2$ (**3**)) ($\lambda_{max} = 400$ nm) [4b], because the absorption bands for $R_2M=MR_2$ ($M = Si$ or Ge) bondings are generally recognized to be in the region $\lambda = 400$ – 430 nm [20]; for example, $Mes_2Ge=GeMes_2$ (406 nm) (W. Ando, H. Itoh, T. Tsumuraya and H. Yoshida, *Organometallics*, **7** (1988) 1880), $Mes_2Si=GeMes_2$ (414 nm) [2c], and $Mes_2Si=SiMes_2$ (420 nm) (R. West, M.J. Fink and J. Michl, *Science*, **214** (1981) 1343).

- [25] W.P. Neumann, *Chem. Rev.*, 91 (1991) 311, and references cited therein.
- [26] G.R. Gillette, G.H. Noren and R. West, *Organometallics*, 8 (1989) 487.
- [27] W. Ando, H. Itoh and T. Tsumuraya, *Organometallics*, 8 (1989) 2759.
- [28] (a) K. Mochida, S. Mori, C. Yoshizawa, S. Tokura, W. Wakasa and H. Hayashi, *J. Organomet. Chem.*, 471 (1994) 47; (b) K. Mochida, K. Kimijima, H. Chiba, M. Wakasa and H. Hayashi, *Organometallics*, 13 (1994) 404.
- [29] H. Watanabe, M. Yoshikawa and Y. Nagai, unpublished work 1988.
- [30] A similar observation has been shown in the photolysis of $\text{Mes}_2\text{Ge}(\text{SiMe}_3)_2$, followed by annealing [27].
- [31] N. Tokitoh, K. Manmaru and R. Okazaki, *J. Chem. Soc. Jpn.*, (1994) 240.
- [32] Compound **13** was probably produced by the reaction of **12** with moisture in the air introduced when the seal of reaction cell was opened.
- [33] H.R. Hudson, *J. Chem. Soc., Perkin Trans. I*, (1976) 754.
- [34] P. Main, S.E. Hull, L. Lessinger, G. Germain, J.P. Declercq and M.M. Woolfson, *MULTAN 78, A System of Computer Programs for the Automatic Solution of Crystal Structures for the X-ray Diffraction Data*, University of York, York; University of Louvain, Louvain; 1978.
- [35] T. Sakurai and K. Kobayashi, *Rikagakukenyujo Houkoku*, 55 (1978) 69.